of the initial antibody repertoire must be removed. Our results establish the initial extent of autoantibody production in healthy individuals and suggest that autoantibody regulation requires two distinct B cell developmental checkpoints. Little is understood about how tolerance is broken in autoimmune diseases in humans, but the finding that large numbers of autoantibodies are produced under physiologic circumstances suggests that even small changes in the efficiency of autoantibody regulation would lead to increased susceptibility to autoimmunity.

**References and Notes**


1. A. M. Silverstein, *Nature Immunol.* **2**, 279 (2001).
2. K. Landsteiner, *The Specificity of Serological Reactions* (Dover, New York, 1936).
3. D. Gay, T. Saunders, S. Camper, M. Weigert, *J. Exp. Med.* **177**, 999 (1993).
4. S. L. Tiegs, D. M. Russell, D. Nemazee, *J. Exp. Med.* **177**, 1009 (1993).
5. D. A. Nemazee, K. Burki, *Nature* **337**, 562 (1989).
6. C. C. Goodnow *et al.*, *Nature* **334**, 676 (1988).
7. See supporting data on *Science* Online.
8. L. G. Billips *et al.*, *Ann. N.Y. Acad. Sci.* **764**, 1 (1995).
9. K. D. Klonowski, L. L. Primiano, M. Monestier, *J. Immunol.* **162**, 1566 (1999).
10. Y. Ichiyoshi, P. Casali, *J. Exp. Med.* **180**, 885 (1994).
11. R. Crouzier, T. Martin, J. L. Pasquali, *J. Immunol.* **154**, 4526 (1995).
12. I. Aguilera, J. Melero, A. Nunez-Roldan, B. Sanchez, *Immunology* **102**, 273 (2001).
13. S. Shiokawa *et al.*, *J. Immunol.* **162**, 6060 (1999).
14. E. Meffre *et al.*, *J. Clin. Invest.* **108**, 879 (2001).
15. M. Z. Radic, M. Weigert, *Annu. Rev. Immunol.* **12**, 487 (1994).
16. S. M. Barbas *et al.*, *Proc. Natl. Acad. Sci. U.S.A.* **92**, 2529 (1995).
17. J. M. Seigneurin, B. Guilbert, M. J. Bourgeat, S. Avrameas, *Blood* **71**, 581 (1988).
18. V. Guigou *et al.*, *J. Immunol.* **146**, 1368 (1991).
19. D. Leslie, P. Lipsky, A. L. Notkins, *J. Clin. Invest.* **108**, 1417 (2001).
20. K. Rajewsky, *Nature* **381**, 751 (1996).
21. A. Rolink *et al.*, *J. Exp. Med.* **178**, 1263 (1993).
22. W. Yu *et al.*, *Nature* **400**, 682 (1999).
23. R. J. Monroe *et al.*, *Immunity* **11**, 201 (1999).
24. R. Kleinfield *et al.*, *Nature* **322**, 843 (1986).
25. M. Reth, P. Gehrmann, E. Petrac, P. Wiese, *Nature* **322**, 840 (1986).
26. M. W. Retter, D. Nemazee, *J. Exp. Med.* **188**, 1231 (1998).
27. R. Casellas *et al.*, *Science* **291**, 1541 (2001).
28. D. Nemazee, M. Weigert, *J. Exp. Med.* **191**, 1813 (2000).
29. L. B. King, J. G. Monroe, *Immunol. Rev.* **176**, 86 (2000).
30. D. M. Allman, S. E. Ferguson, V. M. Lentz, M. P. Cancro, *J. Immunol.* **151**, 4431 (1993).
31. A. G. Rolink, J. Andersson, F. Melchers, *Eur. J. Immunol.* **28**, 3738 (1998).
32. H. Gu *et al.*, *J. Exp. Med.* **173**, 1357 (1991).
33. N. Baumgarth *et al.*, *J. Exp. Med.* **192**, 271 (2000).
34. A. F. Ochsenbein *et al.*, *Science* **286**, 2156 (1999).
35. F. Martin, J. F. Kearney, *Immunol. Rev.* **175**, 70 (2000).



36. We thank K. Velinzon and K. Gordon for help with the single cell sorter, and all members of the Nussenzweig laboratory and E. Besmer for help with the manuscript. Supported by grants from NIH and the Leukemia-Lymphoma Society (M.C.N. and J.W.Y.) and from the Dana Foundation (E.M.). M.C.N. is a Howard Hughes Medical Institute investigator.


**Supporting Online Material**

www.sciencemag.org/cgi/content/full/1086907/DC1
Materials and Methods
Figs. S1 and S2
Tables S1 to S11
References


16 May 2003; accepted 28 July 2003
Published online 14 August 2003;
10.1126/science.1086907
Include this information when citing this paper.


# Allelopathy and Exotic Plant Invasion: From Molecules and Genes to Species Interactions


**Harsh P. Bais,[1] Ramarao Vepachedu,[1] Simon Gilroy,[2] Ragan M. Callaway,[3] Jorge M. Vivanco[1*]**



**Here we present evidence that *Centaurea maculosa* (spotted knapweed), an invasive species in the western United States, displaces native plant species by exuding the phytotoxin (–)-catechin from its roots. Our results show inhibition of native species' growth and germination in field soils at natural concentrations of (–)-catechin. In susceptible species such as *Arabidopsis thaliana*, the allelochemical triggers a wave of reactive oxygen species (ROS) initiated at the root meristem, which leads to a $Ca^{2+}$ signaling cascade triggering genome-wide changes in gene expression and, ultimately, death of the root system. Our results support a "novel weapons hypothesis" for invasive success.**


Invasive plant species threaten the integrity of natural systems throughout the world by displacing native plant communities (*1*) and establishing monocultures in new habitats (*2*). The leading theory for the exceptional success of invasive plants is their escape from the natural enemies that hold them in check, freeing them to utilize their full potential for resource competition (*3*). Allelopathy, the release of phytotoxins by plants, has been proposed as an alternative theory for the success of some invasive plants (*4*). *Centaurea* species are among the most economically destructive exotic invaders in North America, and they have long been suspected of using allelopathic mechanisms to rapidly displace native species (*4*, *5*–*7*). Here we demonstrate the allelopathic effects of *C. maculosa* by integrating ecological, physiological, biochemical, cellular, and genomic approaches.

Previously we have reported the identification of the phytotoxic root exudates from *C. maculosa* (*7*, *8*). The biologically active fraction was found to be racemic catechin: (–)-catechin was phytotoxic, whereas (+)-catechin had antimicrobial properties. Racemic catechin is abundant in soil extracts from *C. maculosa*–invaded fields, supporting the position that *C. maculosa*'s invasiveness is facilitated by (–)-catechin release (*7*). It was observed that (±)-catechin concentration in the soil varied with its proximity to the taproot, differences in soil sampling zones, and age of knapweed's invasion (*7*). We further tested the "novel weapons hypothesis" by measuring the natural concentration of (–)-catechin in rhizospheres in Europe and North America (*9*). (–)-Catechin levels were more than twice as high in soils supporting invasive *C. maculosa* in North America than in Europe (Fig. 1A). Therefore, we analyzed the effect of (–)-catechin on European and North American grasses that interact with *C. maculosa*. The levels of (–)-catechin observed in North American and European soils were added to pots in which three different North American and European grasses were grown separately. When these levels of (–)-catechin were added to natural field soil in pots, the germination and, to a lesser extent, the growth of *Festuca idahoensis* and *Koeleria micrantha*, two native North American grasses, were sharply reduced (*9*) (Fig. 1, B and C). In contrast, both germination and growth data revealed that European grasses were more resistant to (–)-catechin than their North American counterparts (fig. S1). Similar experiments were conducted using *A. thaliana*, which was also negatively affected by (–)-catechin (fig. S2). These results provide strong evidence that the root exudation of (–)-catechin accounts at least in part for the displacement of native plant communities by *C. maculosa*.

For detailed biochemical and molecular analysis of the mode of action of (–)-catechin, we selected *A. thaliana* and *C. diffusa* as target species. *A. thaliana* was chosen to facilitate analysis of genomic responses, whereas *C. diffusa* was selected because it is closely related to *C. maculosa* yet is susceptible to (–)-catechin (*7*). The addition of 100 $\mu g\ ml^{-1}$ (–)-catechin to the roots of *C. dif-*


[1]Department of Horticulture and Landscape Architecture, Cell and Molecular Biology Program, and Graduate Degree Program in Ecology, Colorado State University, Fort Collins, CO 80523, USA. [2]Department of Biology, Pennsylvania State University, University Park, PA 16802, USA. [3]Division of Biological Sciences, University of Montana, Missoula, MO 59812, USA.

*To whom correspondence should be addressed. E-mail: jvivanco@lamar.colostate.edu

*fusa* and *A. thaliana* led to a condensation of the cytoplasm characteristic of cell death (Fig. 2, A to D; fig. S3; Movies S1 and S2). Such alterations in cytoplasmic structure occurred first in the meristematic zone of the root tip and then in the central elongation zone (CEZ) in both species (Fig. 2, A to D). This cytoplasmic condensation was followed by a cascade of cell death proceeding backward up through the stele (Fig. 2, A to D; fig. S3; Movies S1 and S2). To more fully characterize whether this change in cell morphology represented a wave of cell death upon (–)-catechin administration, we followed the pattern of cell death in *C. diffusa* and *A. thaliana* roots using the vital stain fluorescein diacetate (FDA) (*9*). This dye is retained by living cells but leaks from dead cells, rendering them nonfluorescent. Upon (–)-catechin addition, cells from the meristematic and CEZ were affected first and lost viability, shown by loss of FDA fluorescence, 600 s after exposure to the chemical (Fig. 2, E to G; fig. S4). Cells in the mature region of the root were not detectably affected during this time course (Fig. 2F) but died ~55 min later (Fig. 2, F and G). Cell death progressed as a wave along the root and was characterized by sequential loss of viability of individual cells (Fig. 2, F and G). In addition, root hairs showed a termination of cytoplasmic streaming over a 5-min time course, followed by bursting at the apex, but only in hair cells that were undergoing tip growth (Fig. 2, C, D, and H; fig. S5; Movie S3). Root border cells do not appear responsive to (–)-catechin treatment (Fig. 2A; fig. S3). Consistent with its resistance to its own toxin, (–)-catechin had no detectable effect on the viability of the main root axis or growth of root hairs of *C. maculosa* (Fig. 2B; Movies S3 and S4) (*10*).

Plants use sophisticated signal transduction cascades to sense and respond to biotic and abiotic stresses (*11*, *12*). Therefore, we monitored the dynamics of various signaling elements, such as reactive oxygen species (ROS), calcium, and pH, that might be associated with the initial sensing and response to (–)-catechin. ROS production was monitored by imaging the ROS-sensitive fluorescent dye, dichlorofluorescein (DCF), which showed that (–)-catechin induced a rapid (within 10 s) increase in ROS in *C. diffusa* and *A. thaliana* (Fig. 3, A and B; fig. S6) but not in *C. maculosa* (Fig. 3C). The ROS change originated in the meristematic region of the root tip and later moved to the CEZ, suggesting that cells in these regions were the first to sense (–)-catechin. ROS production propagated as a wave through the root apex and then back along the main axis of the root (Fig. 3, A and B; fig. S6; Movie S5). The spatial kinetics of ROS induction are similar to the patterns of cell death induced by (–)-catechin (Fig. 2) but occurred 5 to 10 min before detectable loss of

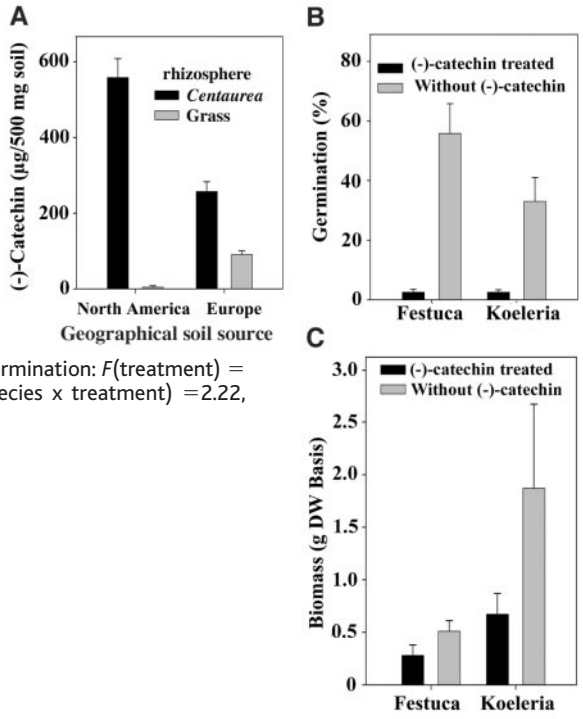


**Fig. 1.** (**A**) Natural concentrations of (–)-catechin in soils supporting invasive *C. maculosa* in North America compared with soils supporting native *C. maculosa* in Europe. Effect of (–)-catechin [200 μg $g^{-1}$ soil dry weight (DW) basis] on the germination (**B**) and total biomass (**C**) of two native North American grasses. Bars, 1 SE. Two-way analysis of variance (ANOVA) for biomass: $F$(treatment) = 16.92, df = 1,39, $P < 0.001$; F(species x treatment) = 9.58, df = 1,39, $P = 0.004$. Two-way ANOVA for germination: $F$(treatment) = 35.47, df = 1,39, $P < 0.001$; $F$(species x treatment) = 2.22, df = 1,39, $P = 0.145$.

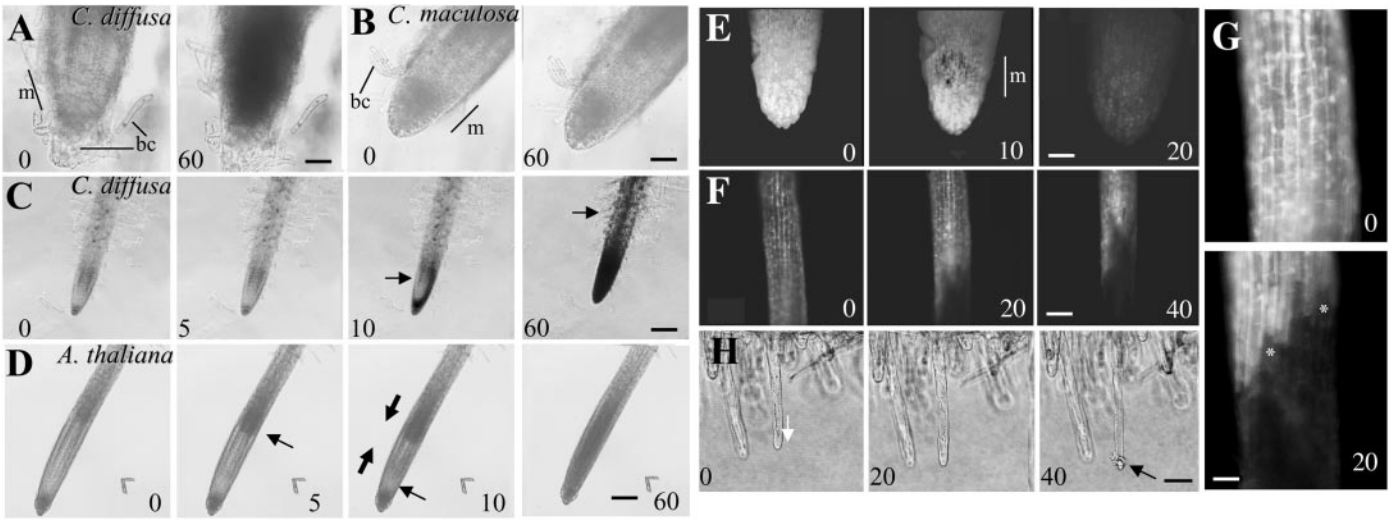


**Fig. 2.** (–)-Catechin (100 μg $ml^{-1}$) elicits a wave of cell death originating in meristematic and CEZ cells of roots of *C. diffusa* and *A. thaliana* but not *C. maculosa* as evidenced by progressive tissue darkening (**A** to **D**) and loss of FDA viability staining (**E** to **G**). bc, border cells; m, meristem. Cell death proceeds as sequential loss of viability of individual cells (*) moving back at approximately 25 μm $min^{-1}$. (**H**) Effect of (–)-catechin (100 μg $ml^{-1}$, added at 20 min) on root hairs of *A. thaliana*. White arrow, growing root hair; black arrow, root hair bursting. The two focal planes at 40 min depict root hair bursting (black arrow). Bars in (A), (B), (E), and (G), 50 μm; in (C) and (D), 150 μm; in (F), 100 μm; and in (H), 20 μm. Images are representative of ≥15 separate roots.

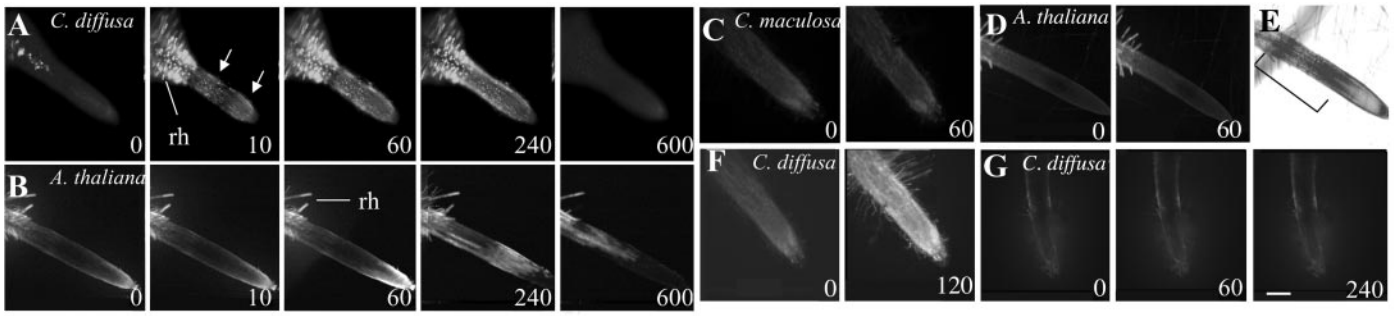


**Fig. 3.** (–)-Catechin (100 μg ml$^{-1}$) elicits intracellular ROS generation in *C. diffusa* (**A**) and *A. thaliana* (**B**), originating at the root tips and progressing back to the elongation zone (arrows) as visualized by dichlorofluorescein (DCF) staining. Note rapid elevation of fluorescence (ROS) in the root hairs (rh). Times represent seconds after treatment. *C. maculosa* (**C**) roots showed low stable levels of ROS (DCF fluorescence) throughout the (–)-catechin treatment. Ascorbic acid (50 mM) resulted in failure of (–)-catechin to induce ROS production in *A. thaliana* (**D**) and *C. diffusa* (**G**) (scale bar, 200 μm), and it kept roots viable (**E**) even at 600 s after catechin treatment. Bracket in (E) indicates the viable CEZ root section. (**F**) *C. diffusa* treated with 25 μM $H_2O_2$ shows uniform increased DCF fluorescence, indicating the patterns of ROS generation seen in (–)-catechin treated roots are unlikely to be an artifact of dye distribution. Images are representative of ≥15 separate roots.

cell viability. In contrast to (–)-catechin, (+)-catechin did not induce ROS change in any of the species tested (*10*). The intracellular concentration of ROS in the root tips and meristematic zone, as measured by assessing oxidation of ferrous ion ($Fe^{2+}$) to ferric ion ($Fe^{3+}$) in vitro (*9*), increased 12-fold within 10 s upon (–)-catechin administration to *A. thaliana* and *C. diffusa* but was unaltered in *C. maculosa* (fig. S7) (*10*). Thus, both DCF-based imaging in vivo and the in vitro quantitative analysis indicated that (–)-catechin elicits a burst of ROS in susceptible plant roots. We therefore attempted to block intracellular ROS production using ascorbic acid (*13*) to characterize its role in the phytotoxicity of (–)-catechin. Ascorbic acid (50 mM) in combination with (–)-catechin (100 μg ml$^{-1}$) blocked the ROS increase seen in response to (–)-catechin (*9*) (Fig. 3, D to G; fig. S6; fig. S7) and the rhizotoxic response (Fig. 3E; fig. S6) in both *C. diffusa* and *A. thaliana*. Therefore, our results indicate (–)-catechin elicits production of ROS that appears required for phytotoxicity and that precedes cell death by 5 to 10 min.

We next determined whether a cytoplasmic $Ca^{2+}$ ($[Ca^{2+}]_{cyt}$)-dependent signaling system (*14*, *15*) was also involved in (–)-catechin action. To image $[Ca^{2+}]_{cyt}$ dynamics, we acid-loaded the roots of *C. diffusa* and *C. maculosa* with the fluorescent $Ca^{2+}$ indicating dye indo-1 (*14*, *15*). For *A. thaliana*, $[Ca^{2+}]_{cyt}$ measurements were made in roots of plants expressing the cameleon YC2.1 green fluorescent protein (GFP)-based $Ca^{2+}$ sensor (*9*). (–)-Catechin treatment resulted in rapid and transient elevations in root tip–localized $[Ca^{2+}]_{cyt}$ levels in *A. thaliana* and *C. diffusa* but not *C. maculosa* seedlings (Fig. 4, A and D; fig. S8). In contrast, (+)-catechin did not induce any detectable change in $[Ca^{2+}]_{cyt}$ in any of the species tested (*10*). In *C. diffusa* and *A. thaliana*, the (–)-catechin–induced increase in $[Ca^{2+}]_{cyt}$ was initiated in the CEZ and meristem 30 s after treatment (Fig. 4) and after the changes in ROS (initiated within 10 s) but before cell death (initiated at 600 s). The mature region of the root showed no $Ca^{2+}$ change over this time frame but did show $Ca^{2+}$ increase at 30 to 40 min, paralleling the delayed cell death seen in this region at 60 min after (–)-catechin treatment (Fig. 4, B and E). The transient elevation in $[Ca^{2+}]_{cyt}$ induced by (–)-catechin only in *A. thaliana* and *C. diffusa* suggests that $Ca^{2+}$ signaling may play a role in the phytotoxic action of (–)-catechin in susceptible species. Ascorbic acid (50 mM) blocked these $Ca^{2+}$ changes, suggesting that the intracellular ROS increase upon (–)-catechin administration is responsible for triggering the $Ca^{2+}$ transient within the cell (fig. S8). Consistent with this idea, extracellular application of $H_2O_2$ produced an increase of $[Ca^{2+}]_{cyt}$ (fig.

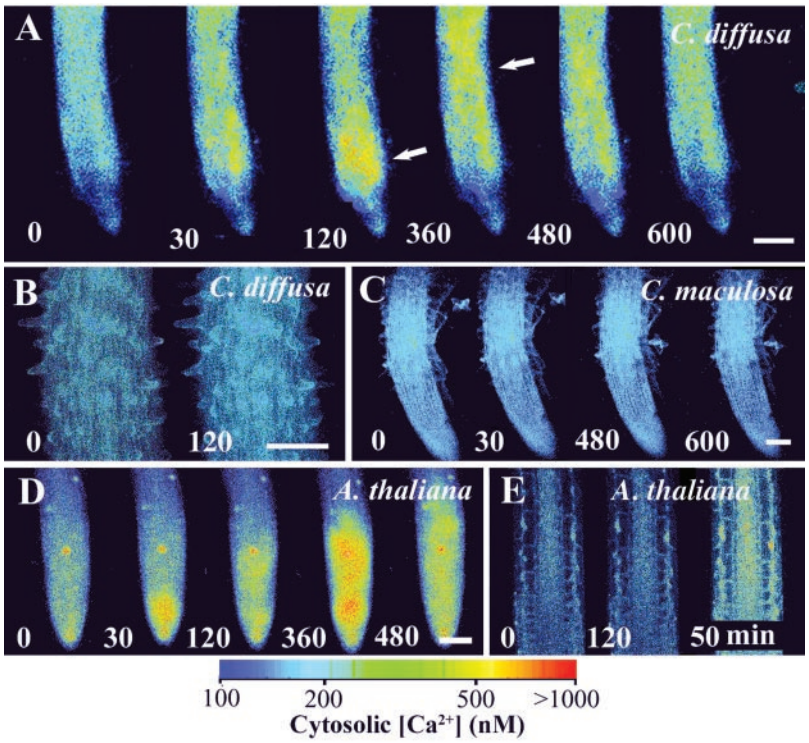


**Fig. 4.** Effect of (–)-catechin (100 μg ml$^{-1}$) on $[Ca^{2+}]_{cyt}$ levels in roots of *C. diffusa* (**A** and **B**), *C. maculosa* (**C**), and *A. thaliana* (**D** and **E**). Roots of *C. diffusa* and *C. maculosa* were acid-loaded with the fluorescent $Ca^{2+}$ indicator indo-1, whereas $Ca^{2+}$ measurements were made in *A. thaliana* using plants expressing the Cameleon YC2.1 GFP-based indicator. Plants were treated with (–)-catechin, and confocal ratio images were taken at the indicated times (s). *C. diffusa* and *A. thaliana* showed a transient elevation in $[Ca^{2+}]_{cyt}$ (arrows) starting approximately 30 s after (–)-catechin treatment in the meristematic region. (A and D) The mature region of the root did not respond, even after almost 1 hour (E). Representative of ≥10 separate roots. $Ca^{2+}$ levels have been pseudocolor coded according to the inset scale. Scale bar represents 200 μm.

S8). Thus, our data are consistent with (–)-catechin eliciting ROS-induced $Ca^{2+}$-dependent events that trigger a program of cell death, initially characterized by loss of ionic homeostasis, such as a failure to maintain cellular pH control (fig. S9).

We next analyzed global gene expression in *Arabidopsis* to define potential transcriptional events associated with (–)-catechin's phytotoxic response (*9*). After 1 hour of treatment with (–)-catechin (100 μg $ml^{-1}$), 956 genes were induced twofold or greater whereas by 12 hours many of these same genes were repressed, likely reflecting the onset of cell death (fig. S10). A large number of these induced genes were related to oxidative stress and the phenylpropanoid and terpenoid pathways (table S1). We also conducted a global gene expression profile 10 min after (–)-catechin treatment to identify possible transcriptional events involved in (–)-catechin signaling or early response. We found a cluster of 10 genes upregulated 10 min after (–)-catechin treatment (fig. S10; table S1). These genes were associated with a steroid sulfotransferase-like protein, α-cystathionase, calmodulin, a ribosomal protein L9, peroxidase ATP21a, a chlorophyll binding protein, and four uncharacterized genes (fig. S10). These genes may be implicated in plant-specific early signal transduction events linked to oxidative stress. It seems likely that acclimation to oxidative stress generated by ROS signaling after (–)-catechin treatment involves concerted, long-term potentiation of different sets of antioxidant and defense genes.

The case we have presented here for allelopathy in *C. maculosa* challenges the conventional ecological perspective that a species' invasiveness is mainly due to enhanced resource competition after escape from natural enemies (*1*) and highlights the role for the biochemical potential of the plant as an important determinant of invasive success.


**References and Notes**

1. T. A. Kennedy *et al.*, *Nature* **418**, 617 (2002).
2. R. M. Callaway, *Trends Ecol. Evol.* **17**, 104 (2002).
3. S. Keane, P. Crawley, *Trends Ecol. Evol.* **17**, 170 (2002).
4. R. M. Callaway, E. T. Aschehoug, *Science* **290**, 521 (2000).
5. S. C. Goslee, D. P. C. Peters, K. G. Beck, *Ecol. Model.* **139**, 31 (2001).
6. W. M. Ridenour, R. M. Callaway, *Oecologia* **126**, 444 (2001).
7. H. P. Bais, T. S. Walker, F. R. Stermitz, R. S. Hufbauer, J. M. Vivanco, *Plant Physiol.* **128**, 1173 (2002).
8. H. P. Bais, V. M. Loyola Vargas, H. E Flores, J. M. Vivanco, *In Vitro Cell. Dev. Biol. Plant* **37**, 730 (2001).
9. Materials and methods are available as supporting material on *Science* online.
10. H. P. Bais, J. M. Vivanco, unpublished data.
11. Z. M. Pei *et al.*, *Nature* **406**, 731 (2000).
12. J. Grant, G. Loake, *Plant Physiol.* **124**, 21 (2000).
13. N. Gheldof, X. Hong Wang, N. J. Engeseth, *J. Agric. Food Chem.* **50**, 5870 (2002).
14. J. M. Fasano *et al.*, *The Plant Cell* **13**, 907 (2001).
15. D. L. Jones, S. Gilory, P. B. Larsen, S. H. Howell, L. V. Kochian, *Planta* **206**, 378 (1998).


16. Supported by grants from Colorado State University Agricultural Experiment Station (J.M.V.), NSF-CAREER (MCB 0093014) (J.M.V.), Invasive Weeds Initiative of the State of Colorado (J.M.V.), and USDA-WRIPM (2003-05060) (J.M.V.), NSF (MCB 02-12099), (S.G.), (NSF DEB-9726829) (R.M.C.), and USDA-NRI (2003-02433) (J.M.V. and R.M.C.).


**Supporting Online Material**

www.sciencemag.org/cgi/content/full/301/5638/1377/DC1
Materials and Methods
Figs. S1 to S10
Table S1
Movies S1 to S5
References

10 February 2003; accepted 1 July 2003

# Nuclear Membrane Proteins with Potential Disease Links Found by Subtractive Proteomics

**Eric C. Schirmer, Laurence Florens,* Tinglu Guan, John R. Yates III,† Larry Gerace†**

**To comprehensively identify integral membrane proteins of the nuclear envelope (NE), we prepared separately NEs and organelles known to cofractionate with them from liver. Proteins detected by multidimensional protein identification technology in the cofractionating organelles were subtracted from the NE data set. In addition to all 13 known NE integral proteins, 67 uncharacterized open reading frames with predicted membrane-spanning regions were identified. All of the eight proteins tested targeted to the NE, indicating that there are substantially more integral proteins of the NE than previously thought. Furthermore, 23 of these mapped within chromosome regions linked to a variety of dystrophies.**

Many diseases have been linked to the nuclear envelope (NE), the membrane structure that forms the boundary of the nuclear compartment (*1*, *2*). The NE contains three distinct functional domains: the outer membrane, a specialized region of the endoplasmic reticulum (ER) that shares properties with rough and smooth ER; the inner membrane, which is lined by the nuclear lamina, a polymer of intermediate filament-type lamin proteins associated with a number of integral membrane proteins; and the nuclear pore complexes (NPCs), which regulate nucleo-cytoplasmic transport of proteins and RNAs. Two integral membrane proteins are localized to the NPC in mammals (*3*), but the number specific to the inner nuclear membrane is unknown: It includes at least 11 proteins and their splice variants (*1*). No proteins specific to the outer membrane have yet been described.

To identify integral proteins of the NE, we took advantage of recent advances in high-throughput shotgun proteomics using multidimensional protein identification technology (MudPIT) (*4*, *5*), by which the coupling of tandem mass spectrometry with multiple liquid chromatography steps allows analysis of the enormous number of peptides generated by direct digestion of a complex biochemical fraction. Eluting peptides are first measured in the ion trap mass spectrometer, then ions are isolated and fragmented by collision-induced dissociation (CID) with the helium bath gas, and the resulting product ions are measured. The fragmentation pattern often yields amino acid sequence information, allowing protein identification from a single unique peptide, thus increasing sensitivity. Avoiding prior separation by polyacrylamide gel electrophoresis removes its chemical and physical biases and the need to solubilize membrane proteins for the analysis (*6*).

To enrich for NE-specific proteins, we employed a "subtractive proteomics" approach (fig. S1). A microsomal membrane (MM) fraction can be prepared devoid of NEs because intact nuclei sediment readily, yet it contains the membranes that contaminate isolated NEs (e.g., mitochondrial membranes) and that are shared between peripheral ER and the NE. Thus, NE-specific proteins were determined by subtracting the proteins present in MM fractions from those of the NE fractions after proteomic analysis.

NEs and MMs isolated from rodent liver (Fig. 1A) (*7*, *8*) were extracted with 0.1 M NaOH to enrich for transmembrane proteins in the pellet (fig. S2). Four times more MMs than NEs were analyzed to increase representation of minor ER proteins. Separately, NEs were extracted with salt and detergent to identify integral proteins more closely associated with the lamin polymer. Although this fraction is expected to contain more intranuclear contaminants, computational sequence analysis should separate those with predicted transmembrane regions. Proteins in all three pellets were proteolytically cleaved, and the complex peptide

Department of Cell Biology, Scripps Research Institute, La Jolla, CA 92037, USA.

*Present address: Stowers Institute for Medical Research, Kansas City, MO 64110, USA.

†To whom correspondence should be addressed. E-mail: lgerace@scripps.edu (L.G.); jyates@scripps.edu (J.R.Y.)